Metal/Ligand-Induced Formation of Metallo-Supramolecular Polymers

J. Benjamin Beck, Jennifer M. Ineman, and Stuart J. Rowan*

The W. M. Keck Laboratories for Organic Synthesis, Department of Macromolecular Science and Engineering, Case Western Reserve University, 2100 Adelbert Road, Cleveland, Ohio 44106-7202

Received February 21, 2005; Revised Manuscript Received April 8, 2005

ABSTRACT: The use of metal−ligand binding as the driving force for the self-assembly polymerizations of a ditopic ligand offers a facile route to the preparation of organic/inorganic hybrid materials. Such metallo-supramolecular polymers potentially offer the functionality of the metal ion along with the processability of a polymer. We report, herein, the preparation and investigation of a series of metallo-supramolecular polymers prepared from three different (macro)monomer units. One monomer has a penta(ethylene glycol) core while the other two consist of poly(tetrahydrofuran) cores of different molecular weights (M_n = 2000 or 4800 g mol^{-1}). Attached to either end of these polyether chains is the terdentate ligand 2,6-bis(benzimidazolyl)-4-oxypyridine. Addition of a metal ion (e.g., Fe(II), Co(II), Zn(II), or Cd(II)), which can bind to the ligand in 1:2 ratio, to a solution of the (macro)monomer results in the self-assembly of linear supramolecular polymers. Viscosity studies demonstrate the formation of self-assembling aggregates and mechanically stable films can be obtained by casting from solution. A series of studies (including DSC, DMA, TGA, and WAXD) were carried out in order to examine the solid-state properties of the films. The metallo-supramolecular polymers, which have the largest poly(tetrahydrofuran) core, form thermoplastic elastomeric films in which the ionic blocks and soft poly(tetrahydrofuran) segments are phase separated.

Introduction

In recent years there has been a growth of interest in the field of supramolecular polymerization,[1−3] i.e., the self-assembly of monomers into polymeric structures through the utilization of the noncovalent bond. One of the easiest conceptual ways of accessing such systems is the placement of "sticky" noncovalent binding motifs onto the chain ends of a bifunctional core unit (Figure 1a). As a consequence, the interactions between these end groups can result in the formation of a supramolecular polymer in which noncovalent bonds are an integral part of the polymeric backbone. Such materials potentially offer an unusual matrix of polymer-like properties. The polymerization is a self-assembly process and as such occurs spontaneously without the need for an initiator (or catalyst). In addition, the presence of noncovalent bonds along the polymeric backbone results in the material exhibiting reversible polymerization/depolymerization characteristics. This behavior, in turn, offers the potential of developing "easy to process" polymeric materials, which, for example, exhibit interesting mechanical, electronic, and/or optical properties.

The properties of such noncovalently bound aggregates have a strong dependence not only on their core components but also on the nature (stability and dynamics) of the supramolecular interactions which control the self-assembly process. Over the years a number of research groups have utilized a variety of different noncovalent interactions, from simple hydrophobic end groups[4−6] to more complex hydrogen bonding motifs,[7−11] to prepare such supramolecular materials. One type of noncovalent bond that offers a large diversity in not only thermodynamic stability but also kinetic lability is that of metal/ligand interactions. Thus, simple addition of metal ions to a monomer that has ligand units placed at either end should result in the self-assembly of metallo-polymeric aggregates (Figure 1b).[12−14] The wide range of possible metal/ligand combinations offers the polymer chemist a wealth of tools with which to tune the properties of these materials by utilizing such coordination chemistry. The degree of interaction (binding constant) between the metal ion and ligand will influence the degree of polymerization of this aggregate. Furthermore, kinetically labile metal/ligand systems should produce "dynamic" polymers which are under continuous equilibrium (cf. supramolecular polymers), while kinetically "inert" metal/ligand combinations will produce polymers similar in nature to the standard covalent systems. Such metallo-supramolecular polymers (sometimes called coordination polymers) also offer the advantage of combining the functionality of the metal ion (e.g., catalysis, luminescence, etc.) with the processing ability of a polymer. In recent years a number of groups have started to investigate the potential that this chemistry has on the formation of such organic/inorganic polymer hybrids utilizing a diverse range of ligands, which include phenanthroline,[15] tetrapyridophenazine,[16,] terpyridine,[17−20] pyridine-2,6-dicarboxylate,[21] porphyrins,[22−25] trialkylphosphines,[26] and pincer ligands.[27]

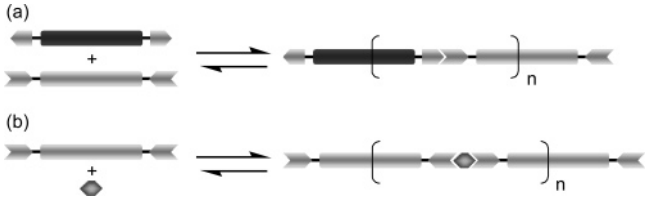

Figure 1. Schematic representations of two supramolecular polymerization processes; formation of (a) an A−A/B−B polymer and (b) a metallo-supramolecular polymer.

Assuming that the polymerization follows a step-growth mechanism and the degree of interaction (or binding constant) between repeat units is independent

* Corresponding author. E-mail: stuart.rowan@case.edu.

10.1021/ma050369e CCC: $30.25
Published on Web 05/12/2005

of molecular weight then the Multi-Stage Open Association Model predicts that the degree of polymerization (DP) is proportional to the square root of the binding constant (K) times the total concentration of components (c):

$$\mathrm{DP} \approx 2(Kc)^{0.5}$$

If the metallo-supramolecular polymers are a two-component A−A/B−B system which consists of ditopic ligand-terminated monomers and metal ions which can bind to only two ligands, then the above prediction for DP would only hold up if the concentration ratio of the components was exactly 1:1. Of course, as with all step-growth polymerizations, deviations from a 1:1 ratio will have a significant negative effect on the overall degree of polymerization. Another major assumption of this model is that no cyclization occurs, and the DP is therefore calculated for the formation of linear aggregates only. Thus, ditopic monomer units which possess identical binding motifs can exhibit very different degrees of polymerization depending on the predisposition of the core to form thermodynamically stable macrocycles.

2,6-Bis(1′-alkylbenzimidazolyl)pyridine is a versatile terdentate ligand that has not only been shown to bind to a range of metal ions[28] but is also very synthetically accessible on large scales. In addition, synthetic procedures to a range of this ligand's derivatives are known which allow tailored functionalization of this binding unit.[29] Recently, we have shown[30−32] that the placement of derivatives of 2,6-bis(1′-methylbenzimidazolyl)-4-oxypyridine (O-Mebip) ligands onto the ends of a monodispersed small core unit (e.g., **1**) can result in the formation of stimuli-responsive metallogels[33] upon the addition of transition metal and/or lanthanoid metal ions. Furthermore, we have shown that 2,6-bis(1′-methylbenzimidazolyl)pyridine (Mebip) ligands can be placed at the ends of conjugated cores to produce light-emitting materials.[34] Binding studies of **1** with Zn^{2+} ions revealed a cooperative effect in the formation of the 2:1 O-Mebip/metal complex as well as a strong overall binding constant (ca. 10^6 M^{-1}).[32] These are both important factors that have been shown by theoretical calculations to aid the formation of supramolecular polymers.[35] We have also recently reported that terminal attachment of simple nucleobase derivatives imparts dramatic changes to the material properties of both low-molecular-weight mesogenic[36] and poly(tetrahydrofuran) core units.[37] We report herein the synthesis and characterization of three ligand-terminated ditopic monomers units, one based on a monodispersed pentaethylene glycol core and the other two on polydispersed low-molecular-weight poly(tetrahydrofuran) telechelic cores, in which 4-oxy-2,6-bis(1′-methylbenzimidazolyl)pyridine derivatives are attached to either chain end. We also examine the polymerization of these ditopic monomers with transition metals and report our initial studies on the characterization of these organic/inorganic hybrid materials.

Experimental Section

Materials. All reagents and solvents were purchased from Aldrich Chemical Co. Reagents were used without further purification. Solvents were distilled from suitable drying agents. Spectrophotometric grade chloroform (filtered over alumina) and acetonitrile were used for all experiments. 4-Hydroxy-2,6-bis(1′-methylbenzimidazolyl)pyridine (**4**) was prepared according to literature procedures.[32]

Instruments. NMR spectra were recorded on a Varian 300 or 600 NMR spectrometer. DSC experiments were carried out on a Perkin-Elmer PYRIS 1 DSC under flowing N_2 at a temperature rate of 10 °C/min. MDSC (modulated) experiments were performed on a TA Instruments DSCQ100 under flowing N_2 at a temperature rate of 3 °C/min. DMA measurements were taken on a Triton Technology Tritec 2000 DMA performing single frequency/strain tension (1 Hz, 0.05 mm) experiments on rectangular films over a temperature scan of 3 °C/min. Thermogravimetric analyses were carried out on a TA Instruments TGAQ500 under N_2. UV−vis spectra were obtained by a Perkin-Elmer Lambda 800 UV−vis spectrometer. Titration experiments were performed in quartz cuvettes scanning in the range of 200−700 nm with an integration time of 0.24 s. Fluorescence spectra were obtained with a SPEX Fluorolog 3 (model FL3-12); corrections for the spectral dispersion of the Xe-lamp, the instrument throughput, and the detector response were applied. Molecular weights of the materials were measured by mass spectrometry on a Bruker BIFLEX III MALDI time-of-flight mass spectrometer using HABA [2-(4-hydroxyphenylazo)benzoic acid] and the matrix with a NaCl additive. The viscosity experiments were performed in a ICL Cannon-Ubbelohde microdilution viscometer using solutions of 0.1 M tetrabutylammonium hexafluorophosphate in chloroform and/or acetonitrile. All viscosity experiments were run at 25 °C in a controlled temperature water bath. X-ray measurements were conducted using a Rigaku SA-HF3 X-ray generator for the D/MAX2000/PC series diffractometer. All samples for X-ray study were prepared as films or powders and placed on a glass cover slide aligned in the path of the wide-angle diffractometer. Fourier transform infrared (FTIR) measurements were conducted on a Bio-Rad FTS-6000 spectrometer using films cast upon CaF_2 disks.

Synthesis of 1. A mixture of **4** (4.85 g, 13.7 mmol) and bisiodopenta(ethylene glycol) (2.5 g, 5.5 mmol) were dissolved into a solution of K_2CO_3 (5.2 g) in 50 mL of DMSO and stirred at 90 °C for 12 h. After removing heat, the mixture was poured into 200 mL of half-saturated NH_4Cl and washed with 100 mL of dichloromethane (3×). The organics were collected and reduced to 5 mL and then extracted again from a mixture of water and dichloromethane. The organics were evaporated and the residue dried in vacuo. The material was purified via column chromatography (silica gel; CH_2Cl_2/MeOH 100:0, 99:1, ..., 97:3) and then precipitated from a 1:1 mixture of dichloromethane and isopropyl ether to yield 2.7 g (54%) of **1** as a white solid; mp 204 °C. ^{1}H NMR (DMSO-d_6): δ 7.92 (4H, s), 7.77 (4H, d, J = 6.7 Hz), 7.68 (4H, d, J = 7.0 Hz), 7.40 (4H, dd, J = 6.9. 8.1 Hz), 7.34 (4H, dd, J = 6.9, 8.1 Hz), 4.43 (4H, t, J = 4.5 Hz), 4.25 (12H, s), 3.86 (4H, t, J = 4.5 Hz), 3.65−3.55 (12H, m). ^{13}C NMR ($CDCl_3$): δ 164.8, 151.9, 149.9, 142.7, 137.5, 124.0, 123.2, 120.5, 111.9, 110.3, 71.4, 70.9, 69.5, 68.1, 32.5. MALDI-MS (matrix: HABA): [M + H] = 914 m/z. UV−vis: λ_{max} = 314 nm. PL ($\lambda_{excitation}$ = 320 nm) $\lambda_{emission}$ = 365 nm.

Synthesis of 5. A mixture of **4** (3 g, 8.45 mmol) and K_2CO_3 (3 g, 20 mmol) was stirred in hot ethanol (90 mL) until it became red in color. Benzyl bromoacetate (2.01 mL, 12.69 mmol) was then added and the solution heated to reflux for 18 h. A mixture of pink solids forms in the reaction flask, and these solids are filtered off and washed with ethanol (1×) and water (3×). The solids were dried under vacuum to yield 3.3 g (95%) of product which did not require further purification. ^{1}H NMR (300 MHz, DMSO-d_6): δ 7.92 (2H, s), 7.81 (2H, d, J = 7.5 Hz), 7.73 (2H, d, J = 7.8 Hz), 7.41 (2H, dd, J = 6.9, 8.1 Hz), 7.34 (2H, dd, J = 6.9, 8.1 Hz), 5.09 (2H, s), 4.29 (6H, s). ^{13}C NMR (300 MHz, DMSO-d_6): δ 169.6, 167.2, 151.1, 150.6, 142.7, 137.8, 123.9, 123.1, 120.2, 112.5, 111.6, 68.7, 33.3. MALDI-MS (matrix: α-cyano-4-hydroxycinnamic acid): m/z 414 $[M + H]^+$.

Synthesis of 2. A mixture of **5** (0.990 g, 2.39 mmol) in dry DMF (10 mL) was stirred for 30 min until fully dissolved. Trimethylacetyl chloride (1.5 mL, 12.19 mmol) was added and the reaction mixture stirred for 10 min. *N*-Methylmorpholine (3.00 mL, 27.26 mmol) and a solution of bis(3-aminopropyl)-

terminated polytetrahydrofuran (**6,** M_n = 2900 g/mol) in DMF (0.45 g, 0.32 mmol, in 5 mL) were then added, and the reaction was allowed to stir for 48 h at room temperature. The DMF was removed under vacuum, and the solids were stirred in chloroform, filtered, and collected. The solution containing the organic fraction was evaporated to dryness, and the resulting solids were purified by column chromatography (silica gel; CH_2Cl_2/MeOH 100:0, 98:2, ..., 90:10) to give 210 mg of **2** (35%). ^{1}H NMR ($CDCl_3$): δ 7.92 (4H, s), 7.85 (4H, d, J = 6.7 Hz), 7.38 (12H, m), 4.74 (4H, s), 4.23 (12H, s), 3.39 (68H, m), 1.61 (64H, m). ^{13}C NMR ($CDCl_3$): δ 166.7, 164.9, 151.9, 150.0, 142.7, 137.5, 124.0, 123.2, 120.5, 111.9, 110.2, 71.3, 70.9, 70.7, 69.6, 67.5, 38.0, 32.8, 29.5, 26.8, 26.7. MALDI-MS (matrix: HABA): M_n = 1725 *m/z*, M_w = 1884 *m/z*, PDI 1.09. FT-IR (cm^{-1}): 1674, 1544, 1595, 1571, 1446, 1477, 1369. UV−vis: λ_{max} = 314 nm. PL ($\lambda_{excitation}$ = 320 nm) $\lambda_{emission}$ = 365 nm.

Synthesis of 3. A mixture of **4** (1.00 g, 2.8 mmol) and triphenylphosphine (1.50 g, 5.7 mmol) was suspended with stirring in 15 mL of freshly distilled THF. 3 mL of diethylazodicarboxylate (DEAD, 40% in toluene) was added to the mixture, resulting in a clear orange solution. Vacuum-dried terathane 2900 (M_n = 2900 g/mol, hydroxyl-terminated polytetrahydrofuran, 3.7 g, 1.3 mmol) in a 10 mL solution of freshly distilled THF was added, and the solution was stirred under an argon atmosphere for 12 h. The tetrahydrofuran was removed in vacuo, and the viscous, lavender residue was redissolved in chloroform. Column chromatography ($CHCl_3$/MeOH, 100:0, 99:1, 98:2, ..., 95:5) resulted in a 0.49 g of a high molecular weight fraction of **3** which is contaminated with some monosubstituted macromonomer (yield 12%) and a 2.48 g fraction of macromonomer **3** (yield 56%). ^{1}H NMR ($CDCl_3$): δ 7.92 (4H, s), 7.85 (4H, d), 7.38 (12H, m), 4.74 (4H, s), 4.23 (12H, s), 3.39 (228H, m), 1.61 (232H, m). ^{13}C NMR ($CDCl_3$): δ 166.6, 151.4, 150.7, 142.8, 137.4, 123.8, 123.1, 120.4, 112.0, 110.2, 70.9, 70.4, 32.8, 26.8. MALDI-MS (matrix: HABA): M_n = 3600 *m/z*. PDI 1.12. UV−vis: λ_{max} = 313 nm. PL ($\lambda_{excitation}$ = 340 nm) $\lambda_{emission}$ = 366 nm.

Typical Sample Preparation of Metallo-Supramolecular Polymers. A solution containing 20.1 mg (0.01 mmol) of **2** in 200 μL of chloroform was mixed with a stoichiometric amount of 3.72 mg (0.01 mmol) of zinc perchlorate hexahydrate in 135 μL of acetonitrile. This mixed solvent solution was then cast onto a glass slide to make a film. The complex was allowed to air-dry and then was vacuum-dried in an oven for 18 h at room temperature. The [**2**·$Zn(ClO_4)_2]_n$ material was then characterized in its solid state or was redissolved in an appropriate solvent to examine its solution properties. The same procedure was used to prepare [**1**·$Zn(ClO_4)_2]_n$ and [**3**·$Zn(ClO_4)_2]_n$ from **1** and **3**, respectively. UV and PL spectra were performed on 0.025 mM (based on moles of ditopic monomer) solutions of each material in acetonitrile. FT-IR was performed on the solid films.

[**1**·$Zn(ClO_4)_2]_n$ FT-IR (cm^{-1}): 1595, 1571, 1477, 1446, 1369, 1100. UV−vis: λ_{max} = 304, 334 nm. PL ($\lambda_{excitation}$ = 340 nm) $\lambda_{emission}$ = 397 nm.

[**2**·$Zn(ClO_4)_2]_n$ FT-IR (cm^{-1}): 1674, 1622, 1606, 1570, 1550, 1490, 1450, 1370, 1100. UV−vis: λ_{max} = 304, 334 nm. PL ($\lambda_{excitation}$ = 340 nm) $\lambda_{emission}$ = 397 nm.

[**3**·$Zn(ClO_4)_2]_n$ FT-IR (cm^{-1}): 1622, 1606, 1568, 1484, 1447, 1371 1115. UV−vis: λ_{max} = 304, 340 nm. PL ($\lambda_{excitation}$ = 340 nm) $\lambda_{emission}$ = 396 nm.

Films suitable for DMA were prepared by casting the metallopolymer solutions onto glass slides in multiple steps. One-third to one-half of the solution is cast and allowed to air-dry. Once dry, a further fraction of the solution is layered upon the freshly formed film and is again allowed to dry. These steps are taken to ensure the films have a thickness greater than 0.10 mm. After vacuum-drying in the oven, making certain there are no trapped air bubbles, rectangular films of uniform thickness can be cut from the center of the thickened films. The trimmings from these films were weighed and redissolved for viscosity experiments and/or cut into smaller pieces suitable for DSC, MDSC, and TGA experiments.

Results and Discussion

Ditopic Monomer Synthesis and Characterization. For this study we focused on two different classes of monomers, which have 2,6-bis(1′-methylbenzimidazolyl)pyridine units attached to either end. The first is a monodispersed ditopic monomer based on a pentaethylene glycol core (**1**) and the second class of materials are polydispersed ditopic monomers based on a polytetrahydrofuran core (**2** and **3**).

The synthesis of the 4-hydroxy-2,6-bis(1′-methylbenzimidazolyl)pyridine ligand (**4**) was achieved in one step, from commercially available starting materials, using literature procedures.[38] The monodispersed ditopic monomer **1** was prepared in one step via the reaction of **1** and bisiodopenta(ethylene glycol) under basic conditions (Scheme 1).[32] The synthetic methodology which we have previously employed[37] for the attachment of supramolecular motifs to polytetrahydrofuran macromonomers is peptide coupling. Thus, we functionalized the hydroxyl group of **4** with benzyl bromoacetate under basic conditions in ethanol to yield directly the acetic acid derivative **5**. The synthesis of the supramolecular telechelic macromonomer **2** was achieved by reacting **5** with the commercially available bis(3-aminopropyl)-terminated polytetrahydrofuran (**6**, M_n = 1400 g mol^{-1}, PDI = 1.10) using mixed anhydride peptide coupling conditions (Scheme 1). This yielded **2** in 35% after purification, and the structure of **2** was confirmed by NMR and MALDI−TOF MS. End-group analysis of the ^{1}H NMR spectrum estimates the molecular weight (M_n) of **2** to be about 2000 g mol^{-1}. This value is in good agreement with the MALDI−TOF MS spectrum, which indicates that the molecular weight (M_n) of **2** is about 1800 g mol^{-1} with a PDI of 1.09. While this methodology worked the yield was not optimal, and it required a macromonomer with amine end groups; thus, we sought an alternative coupling chemistry. Ideally, the direct coupling of the phenolic group on **4** to an alkyl hydroxyl group on the chain end of the polymer would dramatically increase the range of macromonomer units that we could investigate. Thus, we chose to investigate the potential of the Mitsunobu reaction[39] to functionalize the polymer chain ends.[40] Starting with **4** and poly(tetrahydrofuran) (**7**, M_n = 2900 g mol^{-1}) and reacting it with triphenylphosphine and DEAD in THF resulted in desired polymer **3** on a relatively large scale in much better yield. After purification of the reaction mixture by column chromatography we isolated two major fractions. The first fraction corresponds to the ditopic macromonomer **3**, which was obtained in 54% yield, and the second major fraction is a higher molecular weight fraction of **3** contaminated with some monosubstituted poly(tetrahydrofuran). Molecular weight characterization of the first major fraction of the ditopic macromonomer **3** was again carried out using a combination of ^{1}H NMR and MALDI-MS. End-group analysis based on the ^{1}H NMR estimates the M_n of **3** to be around 4800 g mol^{-1}. The MALDI-MS (Figure 2) indicates that the molecular weight (M_n) of **3** is about 3600 g mol^{-1} with a PDI of 1.14. The major peaks in the MALDI-MS correspond to $[M + Na]^+$ with the minor peaks corresponding to either $[M + H]^+$ or $[M + K]^+$. The difference between the NMR and MALDI-MS data for **3** is probably on account of the nature of MALDI-MS experiment which can lead to molecular weight discrimination of the higher molecular weight fraction of a polydispersed sample.[41] It is also important to note that the MALDI−

Scheme 1. Synthesis of the 2,6-Bis(1′-methylbenzimidazolyl)pyridine-Terminated Monomers

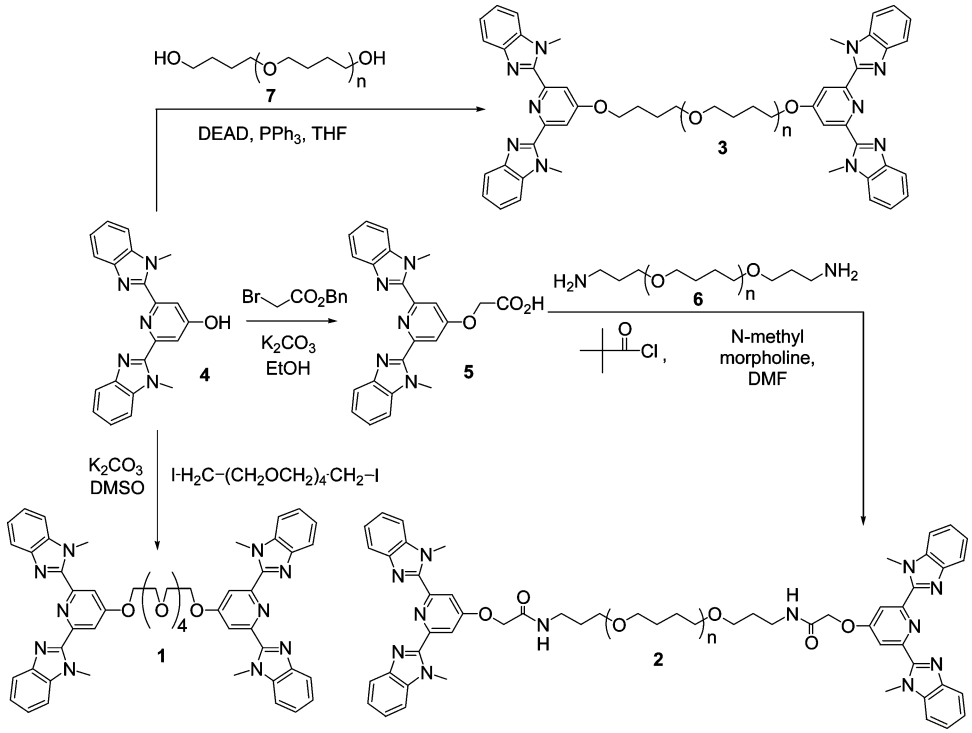

TOF MS of **3** (and also **2**) show no evidence of any monosubstituted material or unreacted starting material.

Self-Assembly and Solution Properties of the Metallo-Supramolecular Polymers. The formation of the metallo-supramolecular materials, $[\mathbf{1}\cdot MX_2]_n$, $[\mathbf{2}\cdot MX_2]_n$, and $[\mathbf{3}\cdot MX_2]_n$, can be achieved by simple addition of 1 equiv of the appropriate metal ion salt to a solution of the ditopic monomer, **1**, **2**, or **3**. We have found that a variety of ions (e.g., Cd^{2+}, Zn^{2+}, Co^{2+}, Fe^{2+}) can be utilized to interact with the terdentate 2,6-bis(1′-methylbenzimidazolyl)-4-oxypyridine (O-Mebip) ligand. The complexation of these metal ions to the ligand can be followed by UV spectroscopy. All the starting materials **1**, **2**, and **3** show the ligand absorption band at 314 nm, which is assigned to the $\pi-\pi^*$ transitions of the ligand. Addition of 1 equiv of either Cd^{2+} or Zn^{2+} ions to any of these monomers in acetonitrile results in a shift of this band to 331 and 334 nm, respectively, but no significant change in the color of the solution. However, addition of either Co^{2+} or Fe^{2+} ions to **1**, **2**, or **3** results in a dramatic change in the color of the solution from colorless to orange or purple, respectively. In the Co^{2+} samples we observe absorption peaks at 306 and 328 nm in acetonitrile along with the presence of weak tailing in the spectra out to around 550 nm, which is assigned to presence of metal-centered d−d transitions and is responsible for the observed orange color of the complexes. In the case of the Fe^{2+} materials absorption peaks are observed at 338, 353, and 568 nm. The purple color of the Fe^{2+} systems occurs as a result of a broad metal-to-ligand charge transfer (MLCT) absorption band around 568 nm, which is indicative of the formation of the 2:1 O-Mebip:Fe^{2+} complex.[42] As mentioned previously, it is important for the self-assembly polymerization process that the stoichiometry of the metal ion and ditopic monomer components is carefully controlled to a monomer: metal ion ratio of 1:1. This can easily be achieved with the monodispersed ditopic monomer **1**; however, it becomes a bit more difficult to calculate the exact stoichiometry with the polydispersed monomers **2** and **3**. We, therefore, carried out a series of titration experiments with either **2** or **3** and $Fe(ClO_4)_2$ in order to confirm the molecular weight of these macromonomers.[43] For these experiments we used the NMR to determine the molecular weight of **2** (M_n = 2000 g mol^{-1}) and **3** (M_n = 4800 g mol^{-1}) as a first approximation. Figure 3 shows the UV spectra of different molar

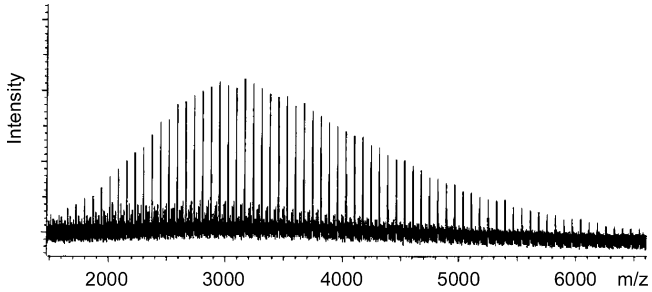

Figure 2. MALDI-MS of **3** with NaCl in a HABA matrix.

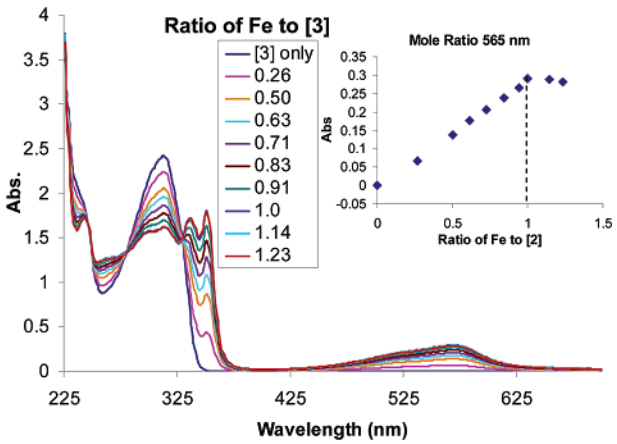

Figure 3. UV titration of $Fe(ClO_4)_2$ into **3** in acetonitrile. Inset: plot of absorbance vs molar ratio of $Fe(ClO_4)_2$ to **3**.

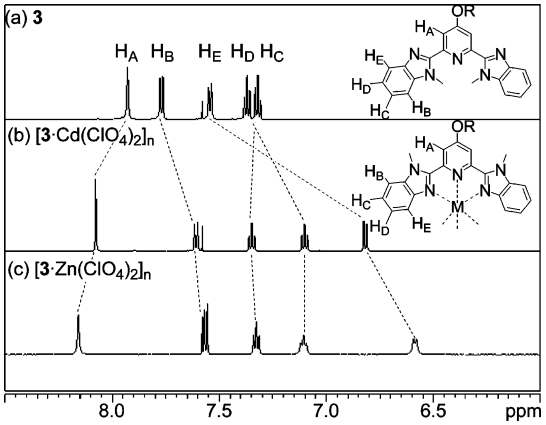

Figure 4. ^{1}H NMR (600 MHz, $CDCl_3$) of the aromatic region of (a) **3**, (b) [**3**·$Cd(ClO_4)_2]_n$, and (c) [**3**·$Zn(ClO_4)_2]_n$.

ratios of $Fe(ClO_4)_2$:**3** in acetonitrile, where we see the growth of the three new peaks which are attributed to the binding of the ligand to Fe^{2+}. The inset shows that the maximum absorbance at 568 nm occurs at an Fe^{2+}:**3** molar ratio of 1:1, based on the M_n of **3** being 4800 g mol^{-1}, and supports the molecular weight estimate determined by NMR end-group analysis. As with the absorption spectra the emission spectra of these systems are also sensitive to metal binding. All the ditopic monomers are fluorescent and show an emission peak at 365 nm in acetonitrile solution. Addition of Zn^{2+} ions to the solution results in a red shift in the emission to 397 nm. Furthermore, the PL titration experiments suggest that most if not all of the ligands are bound to Zn^{2+} at a ratio of 1:1 **3**:$Zn(ClO_4)_2$, even at very dilute concentrations (0.025 mM). Addition of either Fe^{2+} or Co^{2+} ions to any of the monomers results in quenching of the fluorescence of ligand.

Binding of the metal ions to the O-Mebip ligand in solution can also be demonstrated by ^{1}H NMR studies. Figure 4 shows the aromatic region of **3**, [**3**·$Cd(ClO_4)_2]_n$, and [**3**·$Zn(ClO_4)_2]_n$. The assignment of the peaks is based on two-dimensional NMR experiments and literature values.[44] Addition of the metal ions to any of the ditopic monomers results in a number of dramatic shifts of the ^{1}H signals in the aromatic region. The conformation of similar unbound 2,6-bis(1′-alkylbenzimidazolyl)pyridine ligands in both solution and solid-state has the free nitrogens in the benzimidazolyl moiety pointing away from the binding site in order to maximize π-overlap, minimize the repulsion between nitrogen lone pairs, and minimize the dipole moment.[45] Complexation with a metal ion results in a conformational change in the ligand and placement of the H_E proton in close proximity to the binding site. Thus, in the formation of a 2:1 Mebip:metal ion complex the H_E proton on one ligand will be placed close to the aromatic face of the second ligand which should result in this proton being shielded. This is indeed observed as the H_E proton experiences the largest shift upon complexation and is moved upfield by about 0.8−1 ppm.

Having demonstrated from a combination of UV, photoluminescence, and ^{1}H NMR studies the formation of 1:1 monomer-to-metal complexes in solution, the next step was to investigate whether evidence could be obtained for the presence of metallo-supramolecular polymers in solution. The intrinsic viscosity, [η], of a sample is related to the molecular weight M of the polymer through the Mark−Houwink−Sakurada equation: $[\eta] = KM^a$, where K and a are experimentally determined polymer and environmentally specific constants. The K and a values for these materials are not known; however, we can draw some conclusions based on the comparison of the intrinsic viscosity values. To this end, viscosity studies were carried out using a Cannon-Ubbelohde microdilution viscometer, and the relative viscosities of both the starting ditopic ligands (**1**, **2**, or **3**) and their metallo-supramolecular polymers ([**1**·$M(ClO_4)_2]_n$, [**2**·$M(ClO_4)_2]_n$, or [**3**·$M(ClO_4)_2]_n$) were measured at a variety of different concentrations. Initial studies on the metallo-supramolecular polymers in organic solvents showed the presence of the polyelectrolyte effect,[46] namely an increase in the reduced viscosity at high dilution. Therefore, all subsequent viscosity studies were carried out in organic solvents which contain 0.1 M solution of tetrabutylammonium hexafluorophosphate to screen this effect. Most of the viscosity studies were carried out in a combination of 1:1 chloroform/acetonitrile as this solvent was found to dissolve all the materials of interest. The intrinsic viscosity, [η], can be estimated by extrapolation of the reduced viscosity data to where the polymer concentration is zero. Figure 5a shows the Huggins plot (reduced viscosity vs concentration) for all three ditopic monomers and a series of their 1:1 metal ion complexes. For the macromonomers **2** and **3** a significant increase in the intrinsic viscosity is observed upon complexation

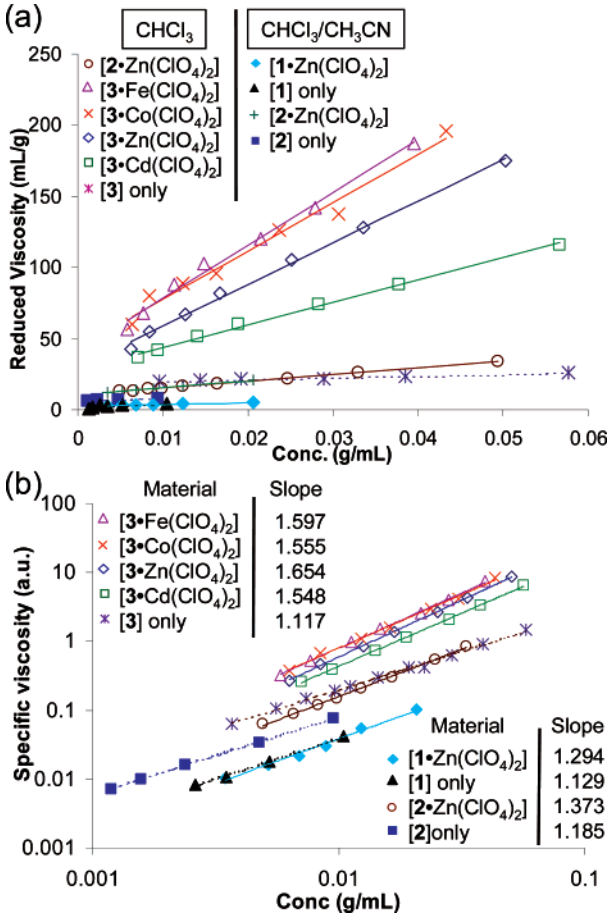

Figure 5. (a) Plot of reduced viscosity vs concentration of for the ditopic monomers **1**, **2**, and **3** and their 1:1 complexes with a selection of metal ions in either chloroform or chloroform/acetonitrile (1:1) containing 0.1 M tetrabutylammonium hexafluorophosphate. (b) Plot of specific viscosity vs concentration with the gradients of the slopes highlighted in the inset (see text).

with 1 equiv of metal ion. For example, an increase in intrinsic viscosity from 6.0 to 10.3 mL/g for **2** and from 18.2 to 30.1 mL/g for **3** is observed upon complexation with $Zn(ClO_4)_2$, which is consistent with the formation of higher molecular weight aggregates. However, for the small monodispersed ligand **1** no significant difference is observed in intrinsic viscosity (2.5 mL/g) for the uncomplexed and Zn^{2+} complexed $[\mathbf{1}\cdot Zn(ClO_4)_2]_n$ systems. Given that the nature of the ligand binding sites is the same in all three systems and that optical spectroscopy indicates that most, if not all, of the ligands are complexed at these concentrations, then the fact that little or no viscosity difference is observed between **1** and $[\mathbf{1}\cdot Zn(ClO_4)_2]_n$ suggests that a significant amount of macrocycles is present in $[\mathbf{1}\cdot Zn(ClO_4)_2]_n$. This can also be seen in Figure 5b, which shows the double-logarithmic plot of specific viscosity vs concentration for the metal complexes of **1**, **2**, and **3**. A linear relationship (i.e., slope of 1) indicates the presence of noninteracting species of a constant size whereas an exponential relationship (slope >1) is consistent with the presence of a supramolecular polymerization process where the size of the aggregate increases with concentration.[47] A slope of 1 can also indicate a significant formation of macrocycles. In fact, there are examples of supramolecular polymeric systems[48] that have been shown to exhibit this linear behavior at low concentrations (which favors the formation of rings) but exhibit an exponential relationship above a critical monomer concentration, which favors the formation of polymers.[49] The viscosities of the free **1**, **2**, and **3** ditopic monomers all show a slope of ca. 1 in the double-logarithmic plot, indicating little or no aggregation behavior in these systems. However, the metal complexes of **1**, **2**, and **3** all show an exponential relationship (1.37−1.65) with specific viscosity vs concentration. Cate's model[47] for an idealized reversible polymer which predicts a larger exponential relationship 3.4−3.7 applies to polymer solutions in the semidilute or concentrated regime, where viscosity is predicted through a reptation model. The concentrations examined for the metallo-supramolecular polymers of **1**, **2**, and **3** are just at or below the overlap concentration for entanglement where viscosity more closely follows the Rouse model and is not dominated by reptation effects. Therefore, a value of 1.6 for the metallo-supramolecular polymers is perfectly reasonable considering the conditions of the experiment. Future work will need to be done at higher concentrations (i.e., >50 mg/mL) to determine whether these systems will emulate the viscosity relationships predicted by the theory for semidilute and concentrated regimes. One reason that might explain the difference observed between the samples is the formation of macrocycles and this is possibly a reason why $[\mathbf{1}\cdot Zn(ClO_4)_2]_n$ exhibits the lowest value of the metallo-supramolecular systems. Other possible reasons for the observed differences could be related to slight mismatches in the stoichiometry of the ditopic monomer and the metal ion in the samples resulting in a slight excess of either of these components, which can then act as a chain terminator.

Solid-State Properties of the Metallo-Supramolecular Polymers. Monomer **1** is a white semicrystalline solid at room temperature, which melts around 204 °C. Addition of $Zn(ClO_4)_2$ to **1** results in a white powdery material upon removal of the solvents. While $[\mathbf{1}\cdot Zn(ClO_4)_2]_n$ does not form mechanically stable films upon solution casting from acetonitrile:chloroform (1:1), fibers of this system can be obtained from the melt at >180 °C.

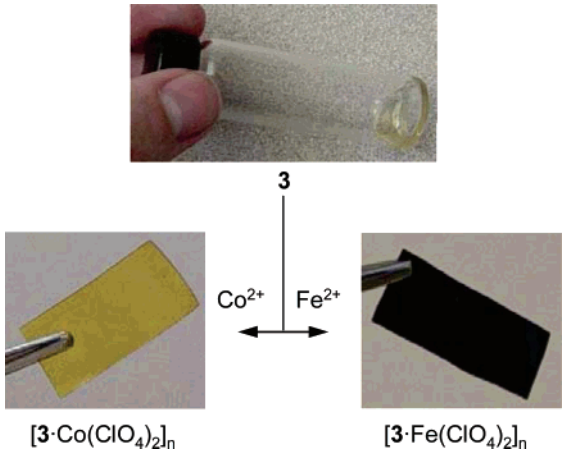

Figure 6. Pictures of the viscous oil **3** and films of the metallo-supramolecular polymers $[\mathbf{3}\cdot Co(ClO_4)_2]_n$ and $[\mathbf{3}\cdot Fe(ClO_4)_2]_n$ which were obtained by solution casting from chloroform solutions.

Table 1. Thermal Data for the Metallo-Supramolecular Polymers of 3[a]

film	T_g (DMA) (°C)	T_c DMA (DSC) (°C)	T_m DMA (DSC) (°C)	TGA 10 wt % loss (°C)
$[\mathbf{3}\cdot Zn(ClO_4)_2]_n$	−80	−41 (−52)	23 (8, 150)	226
$[\mathbf{3}\cdot Cd(ClO_4)_2]_n$	−80	−38 (−52)	26 (8, 153)	214
$[\mathbf{3}\cdot Co(ClO_4)_2]_n$	−76	−45 (−58)	12 (8)	228
$[\mathbf{3}\cdot Fe(ClO_4)_2]_n$	−76	−50 (−58)	12 (8, 149)	311

[a] DMA analysis was carried out on films from −140 to 50 °C at a rate of 3 °C/min, and MDSC was carried out on the same film from −90 to 170 °C also at a rate of 3 °C/min. TGA was carried out under a nitrogen flow at a heating rate of 10 °C/min.

The ditopic macromonomer **2** is a viscous oil at room temperature while **3** will slowly crystallize in the solid state over a period of weeks. **2** shows no discernible endotherms by DSC analysis, while **3** exhibits one endothermic peak upon heating at 22 °C and a crystallization peak at −13 °C upon cooling. Addition of 1 equiv of metal ion to either of these ditopic macromonomers does results in a dramatic change in physical and thermal properties of the materials. For example, all of the 1:1 metal complexes of **2** and **3** that have been studied can be solution processed in to mechanically stable films. Figure 6 shows the examples of the films obtained by solution casting $[\mathbf{3}\cdot Co(ClO_4)_2]_n$ and $[\mathbf{3}\cdot Fe(ClO_4)_2]_n$ from chloroform.

A series of experiments were then carried out in order to better understand the thermal properties of these films, and the data are summarized in Table 1. All the metal ion-containing films of **3** are elastomeric in nature and mechanically stable enough to undergo dynamic thermal mechanical analysis (DMA). Figure 7 shows the results of the DMA experiments. All the samples show a low T_g of around −76 °C (Zn(II) and Cd(II) films) or −80 °C (Co(II) and Fe(II) films), which is close to the reported T_g of −86 °C for poly(tetrahydrofuran). In addition, all the samples also show a slight increase in modulus which maximizes around −40 °C. Modulated differential scanning calorimetry (MDSC) of these films showed an exotherm around this temperature (−52 °C for the Zn(II) and Cd(II) films and −58 °C for the Co(II) and Fe(II) films), indicating that a crystallization event is occurring at these temperatures. A melting

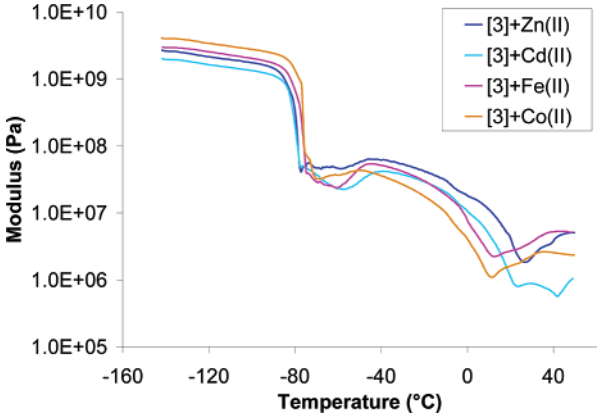

Figure 7. Tensile DMA data of the metallo-supramolecular polymers of **3**.

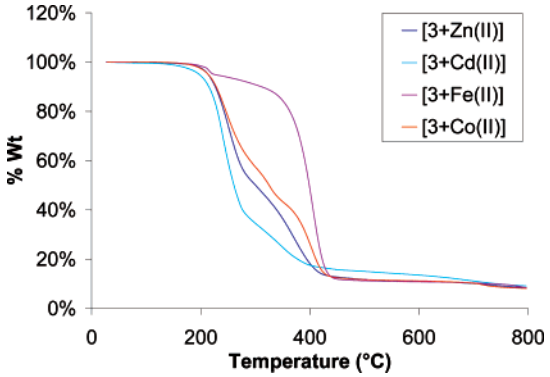

Figure 8. Thermal gravimetric analysis of the metallo-supramolecular polymers of **3** under a nitrogen flow.

temperature is observed on the MDSC for all the samples around 8 °C while the DMA shows a drop in modulus at slightly higher temperatures, which we have assigned to the melting of the semicrystalline poly(THF) segment in the material. This thermal behavior is very similar to those reported for more conventional covalent polyelectrolytes which have poly(THF) segments and been shown to phase separate.[50] Interestingly, above the poly(THF) melting peak an increase in the modulus of all the samples is observed in the DMA. This is rather unusual and suggests some sort of rearrangement process at work here. More work will have to be carried out on these systems to fully elucidate the nature of this process. Finally, the MDSC shows a small endotherm for the Fe(II), Zn(II), and Cd(II) films at 149, 150, and 153 °C, respectively, which corresponds to the T_m of the sample. The presence of what appears to be two T_m's suggests these samples are indeed phase separated. Thermal gravimetric analysis under a nitrogen atmosphere was carried out on these samples (Figure 8). The TGA shows that the metallo-supramolecular polymers show an increased thermal degradation compared to poly(tetrahydrofuran) which starts to degrade at ca. 280 °C.[51] Within the series [**3**·Cd(ClO$_4$)$_2$]$_n$ shows the least thermal stability while [**3**·Fe(ClO$_4$)$_2$]$_n$ exhibits the highest thermal stability. This could be on account of the weaker binding Cd(II) ions decomplexing from the O-Mebip ligand and participating in the metal ion destabilization of the polyether backbone.[51]

The solid-state structures of these materials were investigated by wide-angle X-ray methods. Figure 9a shows the WAXD data for [**1**·Zn(ClO$_4$)$_2$]$_n$, [**2**·Zn(ClO$_4$)$_2$]$_n$, and [**3**·Zn(ClO$_4$)$_2$]$_n$. All three samples show a peak at

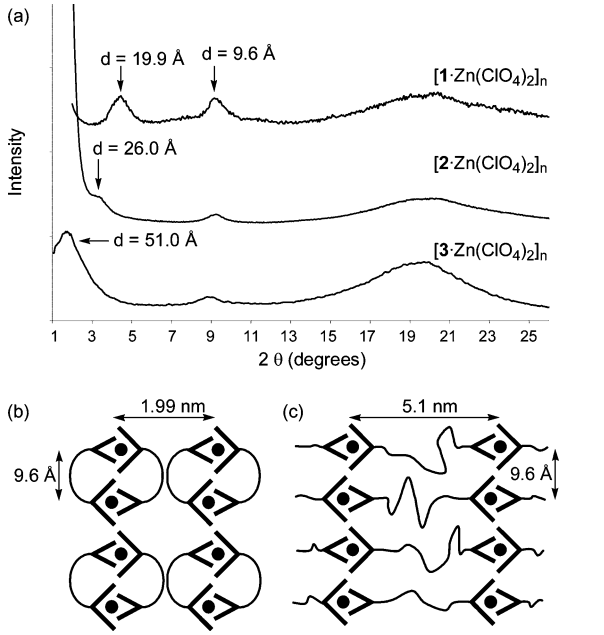

Figure 9. (a) WAXD of films of [**1**·Zn(ClO$_4$)$_2$]$_n$, [**2**·Zn(ClO$_4$)$_2$]$_n$, and [**3**·Zn(ClO$_4$)$_2$]$_n$ and schematic representations of the possible morphologies of (b) [**1**·Zn(ClO$_4$)$_2$]$_n$ and (c) [**3**·Zn(ClO$_4$)$_2$]$_n$.

around $2\theta = 9.36°$, corresponding to a d spacing of 0.96 nm. At lower 2θ we observe a peak that shifts to higher d spacing with increasing soft segment length: $d = 1.99$ nm in [**1**·Zn(ClO$_4$)$_2$]$_n$, 2.60 nm in [**2**·Zn(ClO$_4$)$_2$]$_n$, and 5.10 nm in [**3**·Zn(ClO$_4$)$_2$]$_n$. Finally, there is a broad peak in the region $2\theta = 20°$, which is probably an amorphous halo, although there is small peak at $2\theta = 18.5°$ for [**1**·Zn(ClO$_4$)$_2$]$_n$, which suggests perhaps a higher degree of order than in the two poly(tetrahydrofuran) materials. The first two reflections for each sample are not seen in the unpolymerized monomers and can be assigned to the polymer structures. The existence of a long spacing plus the common reflection $d = 0.96$ nm is suggestive of a layered structure, with the layers increasing in width as the size of the soft polyether segments increases from **1** to **2** to **3**. The reflection at $d = 0.96$ nm is probably due to the packing of the 2:1 Mebip:metal ion complexes, since this dimension is close to the metal-to-metal distance (0.98 nm) observed in the crystal structure of the Mebip$_2$Co(II).[52] No reflections are observed for [**2**·Zn(ClO$_4$)$_2$]$_n$ and [**3**·Zn(ClO$_4$)$_2$]$_n$ that can be assigned to crystalline poly(THF) (predicted at $2\theta = 19.8°$, 24.4°, and 37.7°),[53] so we can conclude that the soft segments are amorphous at room temperature, which is in agreement with the thermal data reported above ($T_m = 8$ °C).

Figure 9b,c shows schematic representations for the layer structures of [**1**·Zn(ClO$_4$)$_2$]$_n$ and [**3**·Zn(ClO$_4$)$_2$]$_n$ that is consistent with the above data. Solution viscosity studies suggest that there is little or no significant molecular weight increase (at the concentrations studied) between **1** and [**1**·Zn(ClO$_4$)$_2$]$_n$, which in turn is indicative of the formation of macrocycles. The observed scattering peaks for [**1**·Zn(ClO$_4$)$_2$]$_n$ are consistent with the formation of layers of a metallo-supramolecular cyclic dimer (Figure 9b). However, it should be noted that from the WAXD data we cannot rule out the possibility of lamella or even once-folded double-lamella structures in the solid state.[18a] In [**3**·Zn(ClO$_4$)$_2$]$_n$ the soft segments are polydisperse, and the actual separation between the ligands will be determined by the need to

fill the available space with the unordered chains. It should be noted that studies on covalent poly(tetrahydrofuran)−polyelectrolyte systems have shown that the latter materials are phase separated into either lamella or hexagonal structures, depending on the length of the poly(THF) segment.[54] For shorter poly(tetrahydrofuran) chain segments ($M_n = (1.8-2.2) \times 10^3$ g mol^{-1}, which corresponds to the size of **2**), lamella structures have been observed, while systems that have longer poly(tetrahydrofuran) segments ($M_n > 3.6 \times 10^3$ g mol^{-1}, which corresponds to the size of **3**), hexagonal structures have been found. Thus, our preliminary studies on these metallo-supramolecular systems are consistent with the formation of phase-separated materials. However, more studies are necessary to determine the detailed structures of these systems.

Conclusion

We have synthesized a series of ditopic monomers which have 2,6-bis(1′-methylbenzimidazolyl)-4-oxypyridine derivatives attached to either end. The self-assembly of metallo-supramolecular polymers occurs upon addition of metal(II) perchlorate salts to these (macro)monomers. Not surprisingly, the nature of the core has a considerable effect on the self-assembly process and consequently the material's properties. The small flexible penta(ethylene glycol) core in **1** encourages the formation of macrocyclic species, and as a result there is little enhancement in the mechanical properties of its metal complexes. However, the metal ion complexes of the macromonomers **2** and **3** do show polymer-like properties both in solution and in the solid state. The properties of these systems are consistent with a phase-separated material which consists of "soft" polyether segments and "hard" ionic segments. Furthermore, it appears that different metal ions do impart slightly different properties onto the metallo-supramolecular polymers, which allows fine-tuning of the properties of these materials. The thermal mechanical data suggest that to some extent this depends on the nature of the metal−ligand interaction with the weaker binding, more labile metal ions (Cd(II), Zn(II)) behaving differently from the stronger binding, less labile metal ions (Co(II), Fe(II)). To summarize, we have demonstrated that the 4-oxy-2,6-bis(benzimidazolyl)pyridine ligand can be used to prepare metallo-supramolecular polymers which show significant enhancement of mechanical properties over the uncomplexed monomers. In addition, we have shown that both the core of the monomers and the nature of the metal ion can be used to control the properties of these self-assembled systems. The wide range of possible cores that can be envisaged, from high-T_g polymers or semicrystalline polymers to conjugated systems, in conjunction with the array of available metal ions, which not only exhibit different binding kinetics and thermodynamics but also can impart functionality, e.g., catalysis, luminescence, etc., opens the door to the creation of easy to process organic/inorganic hybrid materials in which their functionality and mechanical properties can easily be tailored.

Acknowledgment. This material is based upon work supported by the National Science Foundation under Grant CAREER-CHE0133164. The authors of this paper also thank the Case School of Engineering, Dow Chemicals, and the Goodyear Tire and Rubber Co. for financial support of this research. We also thank Prof. J. D. Protasiewicz, Prof. J. Blackwell, and Prof. P. T. Mather for their comments and advice.

Supporting Information Available: Selected NMR, DSC, FT-IR, MALDI-MS, and WAXD data of monomers **1**, **2**, and **3**; UV−vis and photoluminescence spectra of **2** and its complexes with metal ions, MDSC data of the metal ion complexes of **3**, the COSY spectra of C12O-Mebip of the ligand and its complexes with $Cd(ClO_4)_2$, and a movie demonstrating the elastic nature of the $[\mathbf{3}\cdot Zn(ClO_4)_2]_n$. This material is available free of charge via the Internet at http://pubs.acs.org.

References and Notes

(1) Brunsveld, L.; Folmer, B. J. B.; Meijer, E. W.; Sijbesma, R. P. *Chem. Rev.* **2001**, *101*, 4071−4097.
(2) Ciferri, A. *Macromol. Rapid Commun.* **2002**, *23*, 511−529.
(3) *Supramolecular Polymers*, 2nd ed.; Ciferri, A., Ed.; CRC Press, Taylor and Francis: Boca Raton, 2005.
(4) Kastner, U. *Colloids Surf., A* **2001**, *183*−*185*, 805−821.
(5) Yao, N.; Jamieson, A. M. *Polymer* **2000**, *41*, 2925−2930.
(6) Sugiyama, K.; Shiraishi, K.; Matsumoto, T. *J. Polym. Sci., Part A: Polym. Chem.* **2003**, *41*, 1992−2000.
(7) Zimmerman, S. C.; Zeng, F. W.; Reichert, D. E. C.; Kolotuchin, S. V. *Science* **1996**, *271*, 1095−1098.
(8) Castellano, R. K.; Nuckolls, C.; Eichhorn, S. H.; Wood, M. R.; Lovinger, A. J.; Rebek, Jr., J. *Angew. Chem., Int. Ed.* **1999**, *38*, 2603−2606.
(9) Sijbesma, R. P.; Beijer, F. H.; Brunsveld, L.; Folmer, B. J. B.; Hirschberg, J. H. K. K.; Lange, R. F. M.; Lowe, J. K. L.; Meijer, E. W. *Science* **1997**, *278*, 1601−1604.
(10) Xu, J.; Fogleman, E. A.; Craig, S. L. *Macromolecules* **2004**, *37*, 1863−1870.
(11) Binder, W. H.; Kunz, M. J.; Ingolic, E. *J. Polym. Sci., Part A: Polym. Chem.* **2004**, *42*, 162−172.
(12) Constable, E. C. *Chem. Commun.* **1997**, 1073−1080.
(13) Rehahn, M. *Acta Polym.* **1998**, *49*, 201−224.
(14) Lohmeijer, B. G. G.; Schubert, U. S. *J. Polym. Sci., Part A: Polym. Chem.* **2003**, *41*, 1413−1427.
(15) (a) Velten, U.; Rehahn, M. *Chem. Commun.* **1996**, 2639−2640. (b) Velten, U.; Lahn, B.; Rehahn, M. *Macromol. Chem. Phys.* **1997**, *198*, 2789−2816. (c) Velten, U.; Rehahn, M. *Macromol. Chem. Phys.* **1998**, *199*, 127−140. (d) Lahn, B.; Rehahn, M. *Macromol. Symp.* **2001**, *163*, 157−176.
(16) (a) Knapp, R.; Schott, A.; Rehahn, M. *Macromolecules* **1996**, *29*, 478−80. (b) Kelch, S.; Rehahn, M. *Macromolecules* **1997**, *30*, 6185−6193.
(17) (a) Kelch, S.; Rehahn, M. *Macromolecules* **1999**, *32*, 5818−5828. (b) Hinderberger, D.; Schmelz, O.; Rehahn, M.; Jeschke, G. *Angew. Chem., Int. Ed.* **2004**, *43*, 4616−4621.
(18) (a) Schmatloch, S.; van den Berg, A. M. J.; Hofmeier, H.; Schubert, U. S. *Des. Monomers Polym.* **2004**, *7*, 191−201. (b) Hofmeier, H.; Schmatloch, S.; Wouters, D.; Schubert, U. S. *Macromol. Chem. Phys.* **2003**, *204*, 2197−2203. (c) Schmatloch, S.; van den Berg, A. M. J.; Alexeev, A. S. Hofmeier, H.; Schubert, U. S. *Macromolecules* **2003**, *36*, 9943−9949.
(19) (a) El-Ghayoury, A.; Schenning, A. P. H. J.; Meijer E. W. *J. Polym. Sci., Part A: Polym. Chem.* **2002**, *40*, 4020−4023. (b) Dobrawa, R.; Lysetska, M.; Ballester, P.; Grüne, M.; Würthner, F. *Macromolecules* **2005**, *38*, 1315−1325.
(20) (a) Schutte, M.; Kurth, D. G.; Linford, M. R.; Colfen, H.; Mohwald, H. *Angew. Chem., Int. Ed.* **1998**, *37*, 2891−2893. (b) Lehmann, P.; Kurth, D. G.; Brezesinski, G.; Symietz, C. *Chem.*−*Eur. J.* **2001**, *7*, 1646−1651. (c) Kurth D. G.; Severin, N.; Rabe, J. P. *Angew. Chem., Int. Ed.* **2002**, *41*, 3681−3683. (d) Kurth, D. G.; Meister, A.; Thuenemann, A. F.; Foerster, G. *Langmuir* **2003**, *19*, 4055−4057.
(21) (a) Vermonden, T.; van der Gucht, J.; de Waard, P.; Marcelis, A. T. M.; Besseling, N. A. M.; Sudhölter, E. J. R.; Fleer, G. J.; Cohen Stuart, M. A. *Macromolecules* **2003**, *36*, 7035−7044. (b) Vermonden, T.; de Vos, W. M.; Marcelis, A. T. M.; Sudhölter, E. J. R. *Eur. J. Inorg. Chem.* **2004**, *10*, 2847−2852. (c) Vermonden, T.; van Steenbergen, M. J.; Besseling, N. A. M.; Marcelis, A. T. M.; Hennink, W. E.; Sudhoelter, E. J. R.; Cohen Stuart, M. A. *J. Am. Chem. Soc.* **2004**, *126*, 15802−15808.
(22) Michelsen, U.; Hunter, C. A. *Angew. Chem., Int. Ed.* **2000**, *39*, 764−767.
(23) Twyman, L. J.; King, A. S. H. *Chem. Commun.* **2002**, *8*, 910−911.
(24) Ikeda, C.; Fujiwara, E.; Satake, A.; Kobuke, Y. *Chem. Commun.* **2003**, *5*, 616−617.

(25) Nagata, N.; Kugimiya, S.-I.; Fujiwara, E.-I.; Kobuke, Y. *New J. Chem.* **2003**, *27*, 743−747.
(26) Paulusse, J. M. J.; Sijbesma, R. P. *Angew. Chem., Int. Ed.* **2004**, *43*, 4460−4462.
(27) (a) Yount, W. C.; Juwarker, H.; Craig, S. L. *J. Am. Chem. Soc.* **2003**, *125*, 15302−15303. (b) Higley, M. N.; Pollino, J. M.; Hollembeak, E.; Weck, M. *Chem.—Eur. J.*, in press.
(28) For example, see: Piguet, C.; Büenzli, J.-C. G. *Eur. J. Solid State Inorg. Chem.* **1996**, *33*, 165−174.
(29) For example, see: Terazzi, E.; Torelli, S.; Bernardinelli, G.; Rivera, J. P.; Bénech, J.-M.; Bourgogne, C.; Donnio, B.; Guillon, D.; Imbert, D.; Büenzli, J.-C. G.; Pinto, A.; Jeannerat, D.; Piguet, C. *J. Am. Chem. Soc.* **2005**, *127*, 888−903.
(30) Beck, J. B.; Rowan, S. J. *J. Am. Chem. Soc.* **2003**, *125*, 13922−13923.
(31) Zhao, Y.; Beck, J. B.; Rowan, S. J.; Jamieson, A. M. *Macromolecules* **2004**, *37*, 3529−3531.
(32) Rowan, S. J.; Beck, J. B. *Faraday Discuss.* **2005**, *128*, 43−53.
(33) For other recent examples of stimuli responsive metallo-gels see: (a) Kuroiwa, K.; Shibata, T.; Takada, A.; Nemoto, N.; Kimizuka, N. *J. Am. Chem. Soc.* **2004**, *126*, 2016−2021. (b) Kim, H.-J.; Zin, W.-C.; Lee M. *J. Am. Chem. Soc.* **2004**, *126*, 7009−7014. (c) Kawano, S.; Fujita, N.; Shinkai, S. *J. Am. Chem. Soc.* **2004**, *126*, 8592−8593. (d) Kishimura, A. Yamashita, T.; Aida, T. *J. Am. Chem. Soc.* **2005**, *126*, 179−183.
(34) Iyer, P.; Beck, J. B.; Rowan, S. J.; Weder, C. *Chem. Commun.* **2005**, 319−321.
(35) Chen, C. C.; Dormidontova, E. E. *J. Am. Chem. Soc.* **2004**, *126*, 14972−14978.
(36) Sivakova, S.; Rowan, S. J. *Chem. Commun.* **2003**, 2428−2429.
(37) Rowan, S. J.; Suwanmala, P.; Sivakova, S. *J. Polym. Sci., Part A: Polym. Chem.* **2003**, *41*, 3589−3596.
(38) Froidevaux, P.; Harrowfield, J. M.; Sobolev, A. N. *Inorg. Chem.* **2000**, *39*, 4678−4687.
(39) (a) Mitsunobu, O. *Synthesis* **1981**, *1*, 1−28. (b) Hughes, D. L. *Org. React.* **1992**, *42* 335−656.
(40) Mongondry, P.; Bonnans-Plaisance, C.; Jean, M.; Tassin, J. F. *Macromol. Rapid Commun.* **2003**, *24*, 681−685. (b) Skaff, H.; Emrick, T. *Chem. Commun.* **2003**, 52−53.
(41) (a) Nielen, M. W. F. *Mass Spectrom. Rev.* **1999**, *18*, 309−344. (b) Wetzel, S. J.; Guttman, C. M.; Girard, J. E. *Int. J. Mass Spectrom.* **2004**, *238*, 215−225.
(42) Krumholz, P.; Orquima, S. A. *Inorg. Chem.* **1965**, *4*, 612−616.
(43) Johnson, R. M.; Fraser, C. L. *Macromolecules* **2004**, *37*, 2718−2727.
(44) Gelling, A.; Orrell, K. G.; Osborne, A. G.; Šik, V.; Hursthouse, M. B.; Hibbs, D. E.; Malik, K. M. A. *Polyhedron* **1998**, *17*, 2141−2151.
(45) (a) Nozary, H.; Piguet, C.; Tissot, P.; Bernardinelli, G.; Buenzli, J.-C. G.; Deschenaux, R.; Guillon, D. *J. Am. Chem. Soc.* **1998**, *120*, 12274−12288. (b) Nozary, H.; Piguet, C.; Rivera, J.-P.; Tissot, P.; Bernardinelli, G.; Vulliermet, N.; Weber, J.; Buenzli, J.-C. G. *Inorg. Chem.* **2000**, *39*, 5286−5298. (c) Nozary, H.; Piguet, C.; Rivera, J.-P.; Tissot, P.; Morgantini, P.-Y.; Weber, J.; Bernardinelli, G.; Buenzli, J.-C. G.; Deschenaux, R.; Donnio, B.; Guillon, D. *Chem. Mater.* **2002**, *14*, 1075−1090. (d) Terazzi, E.; Torelli, S.; Bernardinelli, G.; Rivera, J.-P.; Benech, J.-M.; Bourgogne, C.; Donnio, B.; Guillon, D.; Imbert, D.; Buenzli, J.-C. G.; Pinto, A.; Jeannerat, D.; Piguet, C. *J. Am. Chem. Soc.* **2005**, *127*, 889−903.
(46) Antonietti, M.; Briel, A.; Foerster, S. *J. Chem. Phys.* **1996**, *105*, 7795−7807.
(47) (a) Ten Cate, A. T.; Sijbesma, R. P. *Macromol. Rapid Commun.* **2002**, *23*, 1094−1112. (b) Cates, M. E. *Macromolecules* **1987**, *20*, 2289−2296.
(48) Ten Cate, A. T.; Kooijman, H.; Spek, A. L.; Sijbesma, R. P.; Meijer, E. W. *J. Am. Chem. Soc.* **2004**, *126*, 3801−3808.
(49) (a) Jacobson, H.; Stockmayer, W. H. *J. Chem. Phys.* **1950**, *18*, 1600−1606. (b) Ercolani, G.; Mandolini, L.; Mencarelli, P.; Roelens, S. *J. Am. Chem. Soc.* **1993**, *115*, 3901−3908.
(50) Grassl, B.; Meurer, B.; Scheer, M.; Galin, J. C. *Macromolecules* **1997**, *30*, 236−245.
(51) Costa, L.; Luda, M. P.; Cameron, G. G.; Qureshi, M. Y. *Polym. Degrad. Stab.* **2000**, *67*, 527−533.
(52) Shklover, V.; Eremenko, I. L.; Berke, H.; Nesper, R.; Zakeeruddin, S. M.; Nazeeruddin, M. K.; Graetzel, M. *Inorg. Chim. Acta* **1994**, *219*, 11−21.
(53) Ikeda, Y.; Murakami, T.; Yuguchi, Y.; Kajiwara, K. *Macromolecules* **1998**, *31*, 1246−1253.
(54) Grassl, B.; Mathis, A.; Rawiso, M.; Galin, J. C. *Macromolecules* **1997**, *30*, 2075−2084.

MA050369E